

RESEARCH

Open Access



Hepatobiliary phase manifestations of breast cancer liver metastasis: differentiating molecular types through Gd-EOB-DTPA-enhanced MRI

Hui Jiang¹, Jin-Rong Qu^{1*}, Li-Feng Wang¹, Peng-Rui Gao¹, Bing-Jie Zheng¹, Hong-Kai Zhang¹ and Li-Na Jiang¹

Abstract

Objective The primary objective of this study is to evaluate the diagnostic efficacy of gadolinium ethoxybenzyl diethylenetriaminepentaacetic acid (Gd-EOB-DTPA) -enhanced magnetic resonance imaging (MRI) in distinguishing breast cancer liver metastasis (BCLM) across different molecular types.

Methods Between August 2014 and July 2021, a cohort of 270 patients histologically diagnosed with BCLM underwent examination through dynamic contrast-enhanced MRI (DCE-MRI). The data collection encompassed clinical information of patients, as well as information on the quantity, shape, boundary, and fusion state of liver metastases. Additionally, MR sequences including T2-weighted imaging with fat suppression (FS), diffusion-weighted imaging (DWI), MR arterial phase, and hepatobiliary phase (HBP) were collected. The chi-squared test was employed to study the correlations between different molecular types of BCLM and imaging features observed in MRI.

Results Significant differences were observed in the HBP image features among various subtypes of breast cancer ($P=0.022$). The morphology (oval, irregular) and fusion state (converging, separated lesions) of BCLM exhibited statistically significant differences based on breast cancer subtypes ($P=0.022, 0.004$). No statistical differences were found in the quantity of BCLM, the boundary of metastasis (clear or vague), and imaging features of the T2WI-FS and DWI concerning the molecular subtypes of BCLM ($P=0.693, 0.161, 0.629, 0.629$).

Conclusion The findings suggest that MRI, particularly Gd-EOB-DTPA-enhanced MRI, they displayed varied enhancement patterns, including the low signal, "target sign", "rim enhancement", and "doughnut-like enhancement". Most basal-like metastases demonstrated a low signal, the other molecular types primarily showing the "target sign". This is invaluable in the imaging diagnosis of BCLM across different molecular type.

Clinical trial number Not applicable.

Keywords Breast cancer, Gd-EOB-DTPA, Liver metastasis, Molecular type, MRI

*Correspondence:

Jin-Rong Qu
jinrongqujr@126.com

¹Department of Radiology, The Affiliated Cancer Hospital of Zhengzhou University & Henan Cancer Hospital, No. 127 Dongming Road, Zhengzhou, Henan Province 450008, China



© The Author(s) 2025. **Open Access** This article is licensed under a Creative Commons Attribution-NonCommercial-NoDerivatives 4.0 International License, which permits any non-commercial use, sharing, distribution and reproduction in any medium or format, as long as you give appropriate credit to the original author(s) and the source, provide a link to the Creative Commons licence, and indicate if you modified the licensed material. You do not have permission under this licence to share adapted material derived from this article or parts of it. The images or other third party material in this article are included in the article's Creative Commons licence, unless indicated otherwise in a credit line to the material. If material is not included in the article's Creative Commons licence and your intended use is not permitted by statutory regulation or exceeds the permitted use, you will need to obtain permission directly from the copyright holder. To view a copy of this licence, visit <http://creativecommons.org/licenses/by-nc-nd/4.0/>.

Introduction

Breast cancer has emerged as one of the most significant malignant conditions affecting women all over the world. Approximately 30–50% of patients may have metastases, notably to the bone, lung, liver, and other organs [1]. As much as 90% of cancer-related fatalities are attributed to metastasis [2]. A consensus was established at the St. Gallen conference in 2011 on the classification of breast cancer at the genetic level, dividing it into four distinct molecular types, namely luminal A, luminal B type, HER-2 type, and basal-like type. This served as a foundation for recommending comprehensive treatment strategies tailored to the specific pathological molecular types of breast cancer. Given the complex pathological features of breast cancer, variations in biological characteristics among different molecular types are substantial. The metastatic sites and prognosis of subtypes of breast cancer are also different: luminal A type has a relatively good prognosis, while the basal-like type has a worse prognosis and a higher rate of brain, lung, and distant nodal metastases [3]. Imaging examinations play an important role in detecting the presence of liver metastasis. However, breast cancer liver metastasis (BCLM) exhibits different manifestations, and the early or atypical manifestations can pose challenges, leading to misdiagnosis or missed diagnoses. In such cases, the definitive diagnosis involves liver puncture.

Imaging manifestations, both direct and indirect, are contingent upon the existence and varied expressions of genes and cytokines. In the hepatobiliary phase (HBP), space-occupying lesions in the liver may exhibit partial or complete high signals. The mechanism can be explained as follows: the contrast agent retains within the extracellular space, depositing in the peritumor region. The retention of gadoxetic acid in the extracellular space is observed in a significant proportion of metastatic carcinomas, ranging from 47 to 70% [4–6]. The observed retention is typically concentrated in the central region of the tumor, indicative of interstitial fibrosis or degeneration. Consequently, this enhancement pattern in the HBP is referred to as the “target sign” (central gadoxetic acid retention in the tumor, indicative of fibrotic stroma or degeneration) [7]. The HBP magnetic resonance imaging (MRI) shows a distinctive “rim” (a hypointense rim during the HBP, resembling the appearance of a capsule on gadoxetic acid-enhanced imaging) or “doughnut-like” enhancement (nodular regenerative hyperplasia shows hyperintensity, with relative hypointensity in the central region of the lesion), attributed to the retention of gadoxetic acid either in the extracellular space or the peritumor region [7].

Hence, a distinct correlation exists between the imaging findings of BCLM and molecular biology, which provides a prerequisite and foundation for investigating the

MRI manifestations associated with different types of BCLM. The objective of this study is to analyze and evaluate the diagnostic efficacy of gadolinium ethoxybenzyl diethylenetriaminepentaacetic acid (Gd-EOB-DTPA)-enhanced MRI in discerning BCLM across various molecular types. By doing so, we aim to provide valuable insights into the clinical diagnosis of the disease, and potentially mitigate the need for unnecessary puncture examinations.

Materials and methods

Study population

Patients who received a histological diagnosis of BCLM at our hospital during the period from August 2014 to July 2021 were chosen for inclusion in this retrospective study. The retrospective study was approved by the Institutional Review Board, and no informed consent was deemed necessary for the use of existing patient data. Inclusion criteria for this study comprised: (1) patients with a confirmed pathological diagnosis of breast cancer; (2) an MRI imaging score of ≥ 3 ; (3) MRI findings indicating liver metastasis, subsequently verified through a biopsy or follow-up. Exclusion criteria for this study comprised: (1) suboptimal image quality with an MRI imaging score < 3 , according to the following criteria: 1 point: The image has many artifacts, severe distortion, and the lesion cannot be detected; 2 points: The image has many artifacts and distortion, allowing partial recognition of the lesion; 3 points: The image quality is fair, with a few artifacts and mild distortion, having a minor impact on diagnosis; 4 points: The image quality is good, with a few artifacts that do not affect diagnosis; 5 points: The image quality is very good. (2) unavailability of complete pathological information. Among 377 eligible patients, 107 patients were excluded—78 patients due to incomplete pathological data and 29 owing to poor image quality. Finally, a total of 270 patients meeting the criteria were included in the study, 126 of whom underwent evaluation through Gd-EOB-DTPA-enhanced MRI, and their data were analyzed subsequently. Figure 1 shows the flow chart depicting the selection process, notably, the distribution of molecular subtypes showed an overrepresentation of patients with the LUMINAL B subtype, exceeding the combined total of the other three subtypes.

All patients underwent a set of routine imaging scans, including MRI (T2WI), diffusion-weighted imaging (DWI), and dynamic contrast-enhanced (DCE) scans. The imaging procedures were conducted on a horizontal table, utilizing a 3.0 Tesla MRI scanner (Skyra; Siemens Healthineers). For the axial scan of DWI (EPI DWI tra), the parameters were (detailed in Table 1): slices:30, slice thickness/slice gap:5.5/0.5 mm, TR:2200ms, TE:51ms, FOV:360 × 360mm², Voxel size:2.65 × 2.65 × 5.5mm³, resolution:108 × 136, NEX:2, TA:35s, breath-hold twice;

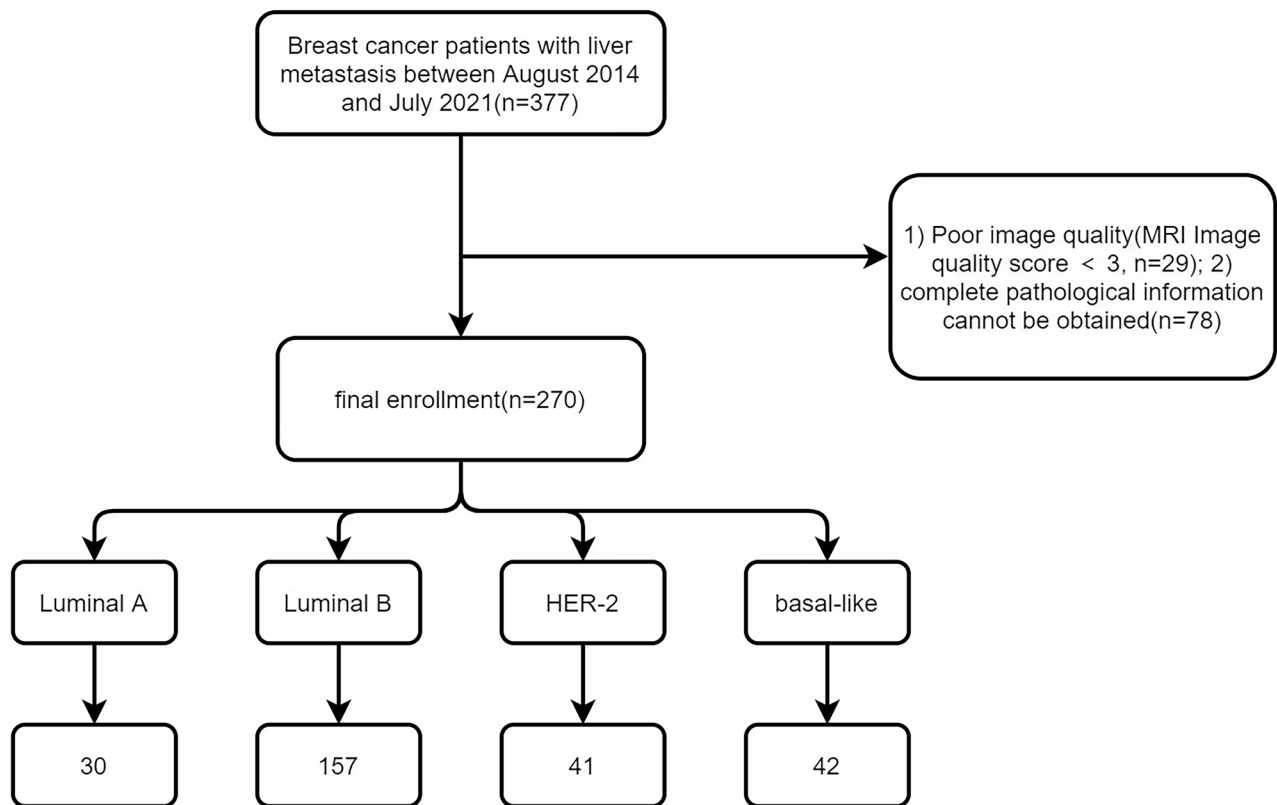


Fig. 1 Flow chart of the study

Table 1 The scan parameters

Protocols	TR / TE (ms)	Slice thickness (mm)	Slices	Flip angle (°)	Base resolution	Phase resolution (%)	FOV (mm)	Voxel size (mm)	Time acquisition
T1WI	4.34 / 1.34	3	120	9	180×288	90	380	0.7×0.7×2.5	18s
T2WI	4000~8000 / 96	5.5	35	133	193×384	70	380	1.0×1.0×5.0	198s
DWI	2600 / 51	5.5	35	—	128×128	100	340	2.7×2.7×7.0	30s
Axial T1 mapping	2.33 / 1.21	5	96	8	83×128	80	380	3.0×3.0×7.0	18s
StarVIBE	3.87 / 1.82	2.5	72	12	168×280	60	380	1.3×1.3×2.5	324s

T2WI-fs: slices:30, slice thickness/slice gap:5.5/0.5 mm, TR:3500ms, TE:83ms, FOV:400×400 mm², Voxel size:1.7×1×5.5 mm³, resolution:151×384, NEX:2, flip angle:140, TA:2min30s, free breathing. T1 twist-vibe Dixon: slices:80, slice thickness:2.5 mm, TR:3.91ms, TE:1.25/2.48ms, FOV:400×400 mm², Voxel size:1.8×1.2×2.5 mm³, resolution:150×320, NEX:1, Flip angle:10, TA:20s(Phase 6)/9S(Phase 1), breath-hold. T1 vibe: slices:88, slice thickness:2.2 mm, TR:3.61ms, TE:1.35ms, FOV:380×380mm², Voxel size:1.44×1.08×4.4 mm³, resolution:190×352, NEX:1, Flip angle:12, TA:15s, breath-hold. The hepatobiliary phase scan was performed at a specific time, i.e. 20 min after the equilibrium phase. For patients with poor liver

function and slow metabolism, the scan was generally performed 40 min later.

Image analysis

All MR images were analyzed by two experienced radiologists, unaware of the patient’s imaging diagnosis and other relevant information. The diagnostic physicians have worked for 11–15 years, and there are also senior physicians with over 20 years of experience, all specializing in the field of liver MRI. In the event of disagreement in the image interpretation, the radiologists were allowed to consult with senior physicians to arrive at a consensus. The following parameters were measured and recorded: MRI manifestations related to the distribution, quantity, size, shape, and boundary of liver metastases,

as well as imaging features in the arterial phase and HBP. Lesion characteristics were assessed across T2WI-FS, DWI, MR-enhanced arterial phase, and HBP images. For statistical analysis, SPSS 22.0 (IBM, New York, USA) was employed. The data were treated as bidirectional disordered enumeration data and were analyzed using the chi-squared test to explore the relationship between two categorical variables. The test level was set at $\alpha=0.05$, with $p<0.05$ indicating statistical differences. To assess the consistency of measurements between the two radiologists the intraclass correlation coefficient (ICC) test was utilized. $ICC<0.2$ indicated poor consistency; ICC in the range of 0.2 to 0.4 indicated general consistency; ICC in the range of 0.4 to 0.6 indicated moderate consistency; ICC in the range of 0.6 to 0.8 indicated strong consistency; and ICC in the range of 0.8 to 1.0 indicated very strong consistency.

Results

Tables 2 and 3, and Fig. 2 present the clinical and pathological features examined in this study. The recorded parameters included age, gender, and pathological classification.

The study revealed a good consistency in the assessment of quantity, shape, boundary and fusion state of BCLM lesions and the foci by the two radiologists across T2WI-FS, DWI, contrast-enhanced MR, and HBP MR images (ICC = 0.97, 0.95, 0.96, 0.98, 0.96, 0.96, 0.91, 0.89).

The study showed that liver metastases predominantly exhibited a pattern of multiple metastases with indistinct

boundaries. Generally, the liver metastases demonstrated a slightly high signal on T2WI-FS and a high signal on DWI. Some liver metastases exhibited features of liquefactive necrosis, presenting as cystic signals (Fig. 3A). A distinctive pattern was observed on DWI, featuring a low signal in the center and a high signal at the boundary, indicating active tumors surrounding necrosis (Fig. 3B). There was no statistical difference found between the quantity of BCLM, the clarity of metastasis boundary (clear or vague), and signal features on T2WI-FS and DWI sequences concerning the molecular types of breast cancer ($P=0.693, 0.161, 0.629, 0.629$).

Liver metastases exhibited diverse shapes, with some being oval, some irregular, and some displaying both oval and irregular characteristics. Metastases in Luminal B and basal-like subtypes were predominantly oval, while metastases in Luminal A and HER-2 subtypes were mostly irregular, and the number of metastases varied greatly among the molecular subtypes. The majority of liver metastases were not fused, with most metastases presenting as isolated entities for all molecular subtypes. The analysis revealed statistical differences in both morphology (oval, irregular) and fusion state (converging, separated lesions) of BCLM concerning the molecular subtypes of breast cancer ($P=0.022, 0.004$).

In this study, the majority of HBP liver metastases exhibited a low signal relative to background liver tissue on the MRI (Fig. 4). They displayed varied enhancement patterns, including the “target sign”, “rim enhancement”, and “doughnut-like enhancement” (Fig. 5). Most basal-like metastases demonstrated a low signal, the other molecular types primarily showing the “target sign”. Statistical analyses revealed significant differences between the imaging manifestations of Gd-EOB-DTPA-enhanced MRI across different subtypes of breast cancer ($P=0.022$).

Table 2 Clinical and pathological characteristics of BCLM

Clinicopathological characteristics	Total (n=270) (proportion, %)
Age (years, mean ± SD)	50 ± 8.7
Gender	
Female	270 (100%)
Group	
BCLMs were found in the first examination	8 (3%)
BCLMs were found by follow-up	262 (97%)
Pathology	
Invasive ductal carcinoma	263 (97.4%)
Invasive lobular carcinoma	2 (0.7%)
Ductal carcinoma in situ	3 (1.1%)
Mucinous carcinoma	1 (0.4%)
Neuroendocrine carcinoma	1 (0.4%)
Molecular types	
Luminal A	30 (11%)
Luminal B	157 (58%)
HER-2	41 (15%)
Basal-like	42 (16%)

Discussion

In this retrospective study, we examined the feasibility and diagnostic value of Gd-EOB-DTPA-enhanced MRI for evaluating BCLM across different molecular types. The results indicated that the majority of HBP liver metastases exhibited a low signal relative to background liver tissue. Most basal-like metastases displayed a low signal, while other types of metastases predominantly showed the “target sign,” with statistical differences observed among them.

Gadoxetic acid is a liver-specific MRI contrast that works through the mediation of organic anion transporting polypeptide 1B3 (OATP1B3) expressed by liver cells. The mixed effect of passive retention of the contrast in the matrix and varying levels of OATP1B3 vector functions can influence the signal intensity changes in oxygenase-enhanced MRI [8, 9]. The reasons for OATP1B3 expression in breast cancer cells remain unclear. In the

Table 3 BCLM-related data

MR characteristics	Luminal A	Luminal B	HER-2	Basal-like	P value
Shape					
Ovoid	18	107	19	28	0.022
Irregular	9	47	21	14	
Both	3	3	1	0	
Boundary					
Clear	14	67	16	24	0.161
Blurred	16	90	25	18	
Fusion					
Converged	9	23	16	9	0.004
Isolated	21	134	25	33	
Number					
Single	6	29	7	11	0.693
Multiple	24	128	34	31	
T2WI-FS					
Slightly hyper-intense	22	100	24	26	0.629
Hyper-intense center surrounded by relatively less intense rim	8	57	17	16	
DWI					
Hyper-intense	22	100	24	26	0.629
Hypo-intense center surrounded with a relatively hyper-intense rim	8	57	17	16	
Arterial phase of contrast- enhanced MRI					
Ring enhancement	19	100	25	30	0.456
Nodular enhancement	4	28	5	4	
Doughnut enhancement	1	8	5	5	
Ring and nodular enhancement	5	20	6	3	
HBP MR					
Hypo-intense	5	15	5	10	0.022
Target sign	5	45	8	8	
Doughnut-like enhancement	3	9	6	5	
Ring-like enhancement	0	2	0	0	

breast cancer cohort, OATP1B3 is significantly associated with a reduced risk of recurrence and improved prognosis [10]. In theory, the basal-like subtype, known for its higher malignancy and lower OATP1B3 expression, is more invasive than other subtypes and is closely linked to distant recurrence, visceral metastasis, and death [11]. Other subtypes of breast cancer tend to have a better prognosis after systematic treatment. In this study, basal like liver metastases exhibit the lowest proportion of mixed signals among all types, potentially linked to the low expression of OATP1B3 in liver metastasis. Further investigation is required to confirm these associations. BCLM with mixed signals may be potentially associated with a better prognosis, warranting future research.

The pathways of liver metastasis include hepatic portal veins, hepatic arteries, and lymph vessels, with veins constituting the primary pathway. Tumors originating from arteries are generally distributed evenly throughout the liver. In the case of breast cancer, metastasis to the liver primarily occurs via the bloodstream through hepatic arteries, resulting in a uniform distribution of liver metastases.

In this study, the majority of liver metastases exhibited blurred boundary, irrespective of molecular subtypes. This may be attributed to the entry of tumor cells into the liver through arteries, where they deposit and grow in arterioles rich in blood supply and strong tumor components. On the T2-weighted fat-suppressed sequence, compared with the surrounding normal liver parenchyma, tumors showed no statistical differences, and the boundaries were blurred. This may be attributed to the inflammatory reactions around the tumor and the reactive hyperplasia of the surrounding fibrous connective tissues. Several studies suggest an association between inflammatory reactions and the metastatic potential of specific tumors in the liver [12, 13].

The predominant shape of the metastatic tumors in this study was oval, which may be attributed to their expansive growth; while irregular shapes may be associated with the rapid progression of lesions. The HER-2 gene, part of the epidermal growth factor receptor family, is considered a proto-oncogene regulating the growth, proliferation, and differentiation of breast cancer cells. Overexpression of HER-2 indicates high malignancy, recurrence, and strong invasiveness and metastasis.

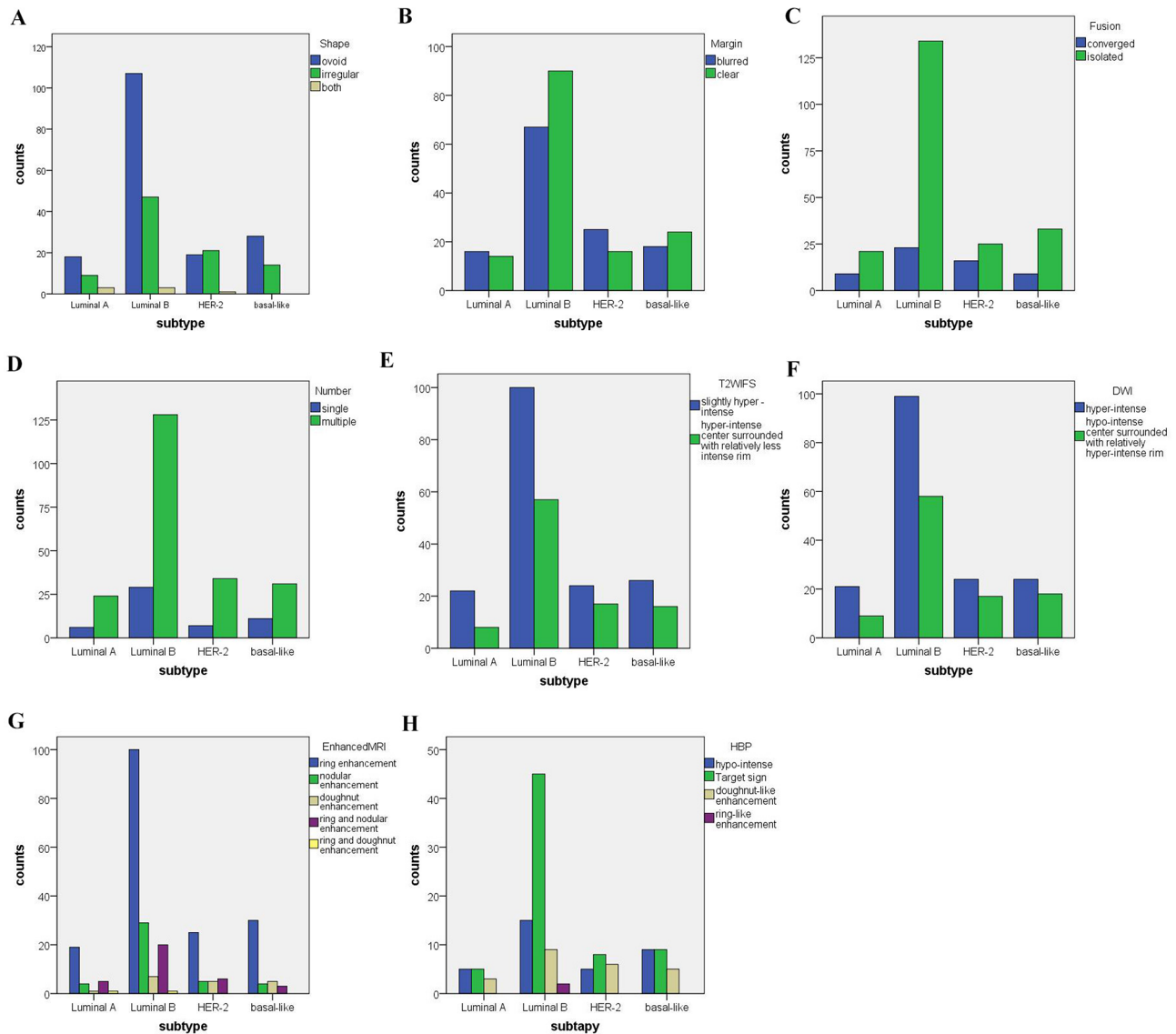


Fig. 2 Statistical results of BCLM-related data

Breast cancer with HER-2 overexpression tends to grow rapidly and exhibit strong invasiveness [14], which may be responsible for the irregular morphology observed in HER-2 liver metastasis. Studies [15, 16] have suggested that A-type breast cancer is common among patients with early breast cancer and has a low recurrence rate. The expression rate of Ki-67 in A-type breast cancer was less than 14%. Gerdes et al. [17] suggested that Ki-67 is a proliferating cell nuclear antigen (PCNA) closely related to the mitosis cycle. Ki-67 only acts in the nucleus of proliferating cells and is not histologically specific. This provides a reliable indicator that comprehensively reflects the proliferative activity of cell populations [18]. The proliferation, metastases, and prognosis of most cancerous lesions are related to the expression of Ki-67. There exists a positive correlation between the expression of Ki-67

and the histological grade of the tumor. Higher levels of Ki-67 expression are indicative of poorer differentiation of tumor tissue. In theory, Luminal A type breast cancer should exhibit a higher prevalence of oval metastases; however, in our study, we observed a contrary outcome, potentially attributed to the limited sample size and a higher proportion of patients with Luminal B breast cancer compared to other types. The biological and genetic heterogeneity [19, 20] in breast cancer, and changes in some biological features during tumor progression may contribute to differences between the biological features of metastatic lesions and primary lesions.

Most foci were isolated in this study, which could be attributed to the fact that most of the cases we included were first-time diagnoses of liver metastases, potentially influencing the data. Studies have found that ER+ breast

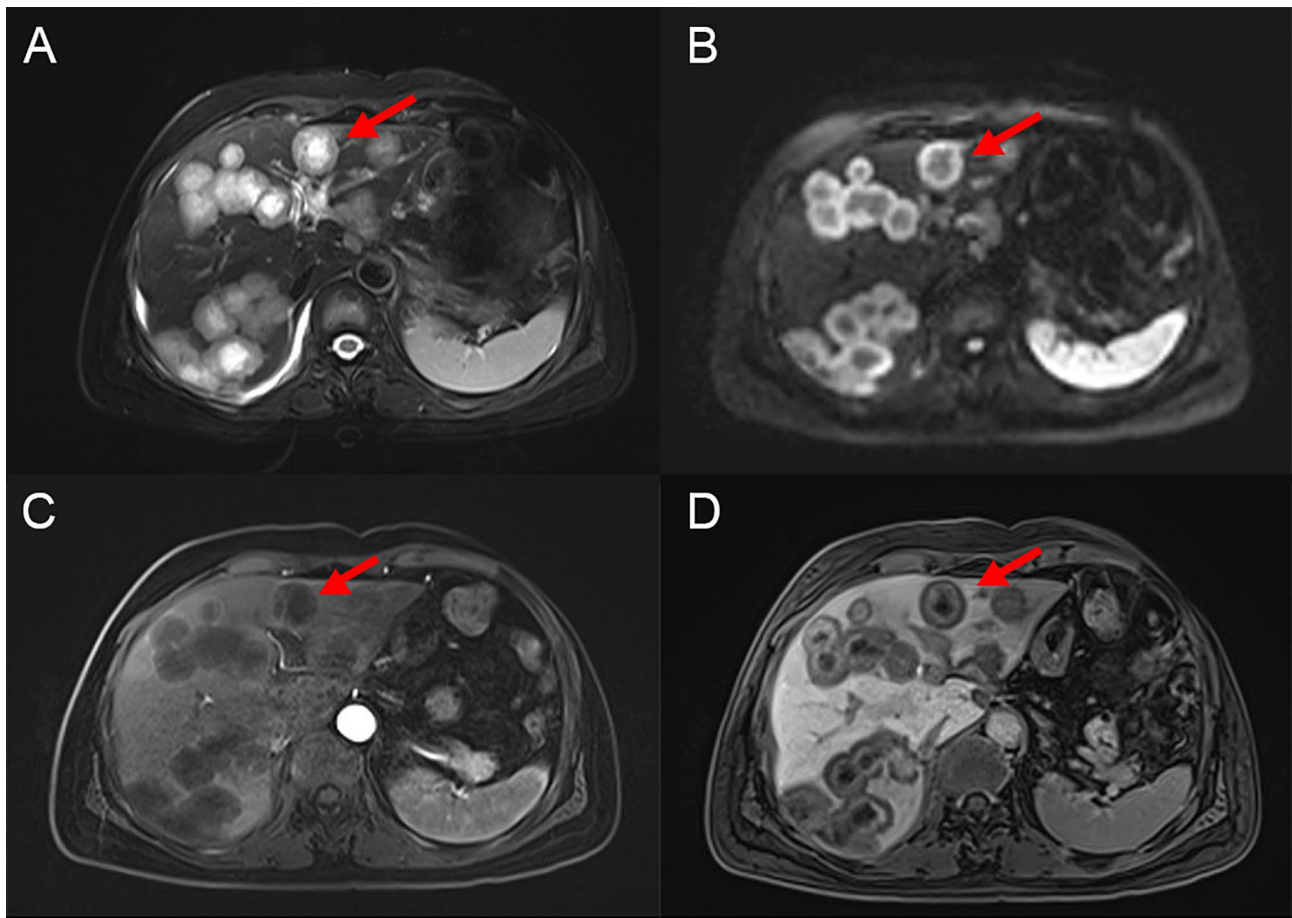


Fig. 3 A patient with invasive ductal carcinoma, of the basal-like subtype. **(A)** T2WI-FS sequence: Lesion center (arrow) shows hyper-intense. Edge exhibits slightly low signal. **(B)** DWI sequence: Lesion center (arrow) shows hypo-intense. Edge shows slightly hyper-intense. **(C)** Arterial phase of contrast-enhanced MRI: Tumor boundary exhibits edge enhancement (arrow), characterized as rim enhancement. **(D)** Axial MR image of HBP: Axial HBP MR image shows the tumor (arrows) with hyperintense areas owing to the retention of gadoteric acid in the extracellular space. It manifests as doughnut-like enhancement and multiple fusion foci



Fig. 4 A patient with invasive ductal carcinoma, of Luminal B sub-type. **(A)** T2WI-FS sequence: Lesion (arrow) shows slightly a hyper-intense signal. **(B)** DWI sequence: Lesion (arrow) shows hyper-intense (ADC: $1.0 \times 10^{-3} \text{ mm}^2/\text{s}$). **(C)** Axial MR image of HBP: Lesion (arrow) shows a hypo-intense signal

cancer is highly differentiated, while ER- breast cancer is poorly differentiated [21], and ER is positively expressed in Luminal B breast cancer and negatively expressed in HER-2 and basal-like breast cancers. Our study showed a higher proportion of fusion foci in HER-2 breast cancer compared to other types, likely due to its high malignancy and rapid growth (Fig. 3A-D). However, the

findings related to the basal-like subtype in this study did not align with expectations, particularly the observation that basal-like lesions tend to be more solitary rather than fused, as is generally seen with rapidly growing malignant lesions. This discrepancy may be due to the small sample size and the biological and genetic heterogeneity of breast cancer, which could have influenced the observed

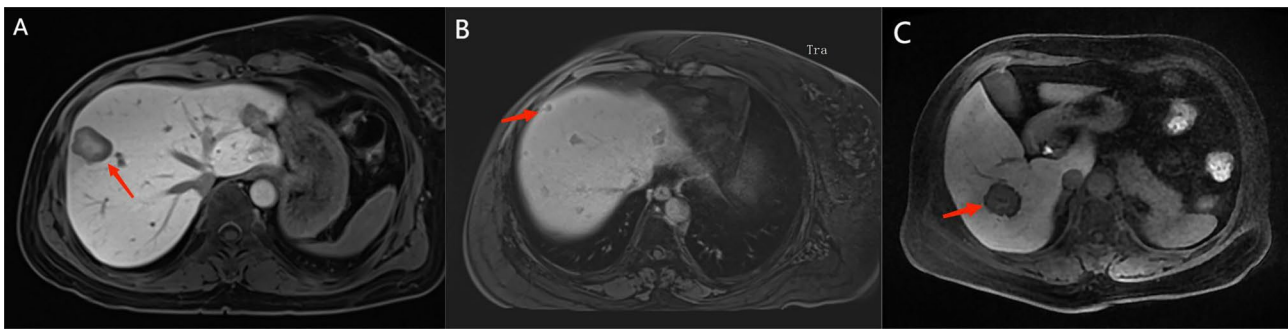


Fig. 5 (A) A patient with invasive ductal carcinoma, Luminal B subtype. Axial MR image of HBP: Lesion (arrow) shows “target sign”. (B) 58-year-old female with invasive ductal carcinoma, HER2 sub type. Axial MR image of HBP: Lesion (arrow) shows rim enhancement. (C) 66-year-old female with invasive ductal carcinoma, Luminal B subtype. Axial MR image of HBP: Lesion (arrow) shows “doughnut-like” enhancement

patterns of lesion growth and metastasis. Changes in certain biological features during tumor progression may lead to differences between the biological characteristics of the metastatic lesions and the primary lesions.

This study is subject to certain limitations, notably the small sample size, which may compromise the accuracy of certain findings and influence the overall results. A recommendation for future research includes expanding the sample size to enhance precision. Additionally, the exclusion of cases with incomplete clinical data led to an unbalanced distribution of molecular subtypes, particularly with an overrepresentation of the LUMINAL B subtype. This imbalance may have impacted the analysis results and should be considered when interpreting the findings.

Conclusion

In this study, the findings suggest that MRI, particularly Gd-EOB-DTPA-enhanced MRI, displayed varied enhancement patterns, including the low signal, “target sign”, “rim enhancement”, and “doughnut-like enhancement”. Most basal-like metastases demonstrated a low signal, the other molecular types primarily showing the “target sign.” This is invaluable in the imaging diagnosis of BCLM across different molecular type.

Abbreviations

BCLM	Breast cancer liver metastasis
HBP	Hepatobiliary-phase
FS	Fat suppression
DWI	Diffusion Weighted Imaging
Gd-EOB-DTPA	Gadolinium-ethoxibenzyl-diethylenetriamine pentaacetic acid

Author contributions

Hui Jiang conceptualized the study, collected the data, and drafted the manuscript. Jin-Rong Qu conceptualized the study and edited the manuscript. Li-Feng Wang interpreted and analyzed the data. Peng-Rui Gao collected and analyzed the data. Bing-Jie Zheng drafted and edited the manuscript. Hong-Kai Zhang and Li-Na Jiang drafted the manuscript and provided technical support. All authors read and approved the final draft.

Funding

No external funding was received to conduct this study.

Data availability

The datasets used and/or analyzed during the current study are available from the corresponding author upon reasonable request.

Declarations

Ethical approval

This study was conducted with approval from the Ethics Committee of The Affiliated Cancer Hospital of Zhengzhou University & Henan Cancer Hospital (No. HNCH-HER2-MBC001). This study was conducted in accordance with the declaration of Helsinki. Since this study is retrospective and does no harm to the participants and only reviews the data, informed consent was exempted.

Consent for publication

Not applicable.

Competing interests

The authors declare no competing interests.

Received: 29 September 2024 / Accepted: 20 March 2025

Published online: 28 March 2025

References

- van Walsum GA, de Ridder JA, Verhoef C, Bosscha K, van Gulik TM, Hesselink EJ, Ruers TJ, van den Tol MP, Nagtegaal ID, Brouwers M, van Hillegersberg R, Porte RJ, Rijken AM, Strobbe LJ, de Wilt JH, Dutch Liver Surgeons Group. Resection of liver metastases in patients with breast cancer: survival and prognostic factors. *Eur J Surg Oncol*. 2012;38(10):910–7. <https://doi.org/10.1016/j.ejso.2012.04.015>.
- Cancer Genome Atlas Network. Comprehensive molecular portraits of human breast tumors. *Nature*. 2012;490(7418):61–70. <https://doi.org/10.1038/nature11412>.
- Kennecke H, Yerushalmi R, Woods R, Cheang MC, Voduc D, Speers CH, Nielsen TO, Gelmon K. Metastatic behavior of breast cancer subtypes. *J Clin Oncol*. 2010;28(20):3271–7. <https://doi.org/10.1200/JCO.2009.25.9820>.
- Ha S, Lee CH, Kim BH, Park YS, Lee J, Choi JW, Kim KA, Park CM. Paradoxical uptake of Gd-EOB-DTPA on the hepatobiliary phase in the evaluation of hepatic metastasis from breast cancer: is the target sign a common finding? *Magn Reson Imaging*. 2012;30(8):1083–90. <https://doi.org/10.1016/j.mri.2012.03.007>.
- Kim A, Lee CH, Kim BH, Lee J, Choi JW, Park YS, Kim KA, Park CM. Gadoteric acid-enhanced 3.0T MRI for the evaluation of hepatic metastasis from colorectal cancer: metastasis is not always seen as a defect in the hepatobiliary phase. *Eur J Radiol*. 2012;81(12):3998–4004. <https://doi.org/10.1016/j.ejrad.2012.03.032>.
- Granata V, Catalano O, Fusco R, Tatangelo F, Rega D, Nasti G, Avallone A, Piccirillo M, Izzo F, Petrillo A. The target sign in colorectal liver metastases: an atypical Gd-EOB-DTPA uptake on the hepatobiliary phase of MR imaging. *Abdom Imaging*. 2015;40(7):2364–71. <https://doi.org/10.1007/s00261-015-0488-7>.

7. Fujita N, Nishie A, Asayama Y, Ishigami K, Ushijima Y, Kakiyama D, Nakayama T, Morita K, Ishimatsu K, Honda H. Hyperintense Liver Masses at Hepatobiliary Phase Gadolinic Acid-enhanced MRI: Imaging Appearances and Clinical Importance. *Radiographics*. 2020 Jan-Feb;40(1):72–94. <https://doi.org/10.1148/rg.2020190037>
8. Briz O, Serrano MA, Maclas RI, Gonzalez-Gallego J, Marin JJ. Role of organic anion-transporting polypeptides, OATP-A, OATP-C, and OATP-8, in the human placenta-maternal liver tandem excretory pathway for fetal bilirubin. *Biochem J*. 2003;371(Pt 3):897–905. <https://doi.org/10.1042/BJ20030034>.
9. Cui Y, König J, Leier I, Buchholz U, Keppler D. Hepatic uptake of bilirubin and its conjugates by the human organic anion transporter SLC21A6. *J Biol Chem*. 2001;276(13):9626–30. <https://doi.org/10.1074/jbc.M004968200>.
10. Muto M, Onogawa T, Suzuki T, Ishida T, Akiyama T, Katayose Y, Ohuchi N, Sasano H, Abe T, Unno M. Human liver-specific organic anion transporter-2 is a potent prognostic factor for human breast carcinoma. *Cancer Sci*. 2007;98(10):1570–6. <https://doi.org/10.1111/j.1349-7006.2007.00570.x>.
11. Anders CK, Carey LA. Biology, metastatic patterns, and treatment of patients with triple-negative breast cancer. *Clin Breast Cancer*. 2009;9(Suppl 2):S73–81. <https://doi.org/10.3816/CBC.2009.s.008>.
12. St Hill CA. Interactions between endothelial selectins and cancer cells regulate metastasis. *Front Biosci (Landmark Ed)*. 2011;16(9):3233–51. <https://doi.org/10.2741/3909>.
13. Khatib AM, Fallavollita L, Wancewicz EV, Monia BP, Brodt P. Inhibition of hepatic endothelial E-selectin expression by C-raf antisense oligonucleotides blocks colorectal carcinoma liver metastasis. *Cancer Res*. 2002;62(19):5393–8.
14. Laganière J, Deblois G, Lefebvre C, Bataille AR, Robert F, Giguère V. From the cover: location analysis of Estrogen receptor alpha target promoters reveals that FOXA1 defines a domain of the Estrogen response. *Proc Natl Acad Sci U S A*. 2005;102(33):11651–6. <https://doi.org/10.1073/pnas.0505575102>.
15. Schnitt SJ. Will molecular classification replace traditional breast pathology? *Int J Surg Pathol*. 2010;18(3 Suppl):S162–6. <https://doi.org/10.1177/1066896910370771>.
16. Zhao J, Liu H, Wang M, Gu L, Guo X, Gu F, Fu L. Characteristics and prognosis for molecular breast cancer subtypes in Chinese women. *J Surg Oncol*. 2009;100(2):89–94. <https://doi.org/10.1002/jso.21307>.
17. Gerdes J, Schwab U, Lemke H, Stein H. Production of a mouse monoclonal antibody reactive with a human nuclear antigen associated with cell proliferation. *Int J Cancer*. 1983;31(1):13–20. <https://doi.org/10.1002/ijc.2910310104>.
18. Viale G, Giobbie-Hurder A, Regan MM, Coates AS, Mastropasqua MG, Dell'Orto P, et al. Breast international group trial 1–98. Prognostic and predictive value of centrally reviewed Ki-67 labeling index in postmenopausal women with endocrine-responsive breast cancer: results from breast international group trial 1–98 comparing adjuvant Tamoxifen with letrozole. *J Clin Oncol*. 2008;26(34):5569–75. <https://doi.org/10.1200/JCO.2008.17.0829>.
19. Amir E, Clemons M, Purdie CA, Miller N, Quinlan P, Geddie W, Coleman RE, Freedman OC, Jordan LB, Thompson AM. Tissue confirmation of disease recurrence in breast cancer patients: pooled analysis of multi-centre, multi-disciplinary prospective studies. *Cancer Treat Rev*. 2012;38(6):708–14. <https://doi.org/10.1016/j.ctrv.2011.11.006>.
20. Sari E, Guler G, Hayran M, Gullu I, Altundag K, Ozisik Y. Comparative study of the immunohistochemical detection of hormone receptor status and HER-2 expression in primary and paired recurrent/metastatic lesions of patients with breast cancer. *Med Oncol*. 2011;28(1):57–63. <https://doi.org/10.1007/s12032-010-9418-2>.
21. International Breast Cancer Study Group, Colleoni M, Gelber S, Goldhirsch A, Aebi S, Castiglione-Gertsch M, Price KN, Coates AS, Gelber RD. Tamoxifen after adjuvant chemotherapy for premenopausal women with lymph node-positive breast cancer: international breast cancer study group trial 13–93. *J Clin Oncol*. 2006;24(9):1332–41. <https://doi.org/10.1200/JCO.2005.03.0783>.

Publisher's note

Springer Nature remains neutral with regard to jurisdictional claims in published maps and institutional affiliations.